Hybrid Interweave-Underlay Millimeter-Wave Spectrum Access in Multi-Operator Cognitive Radio Networks Toward 6G

Rony Kumer Saha
Radio and Spectrum Laboratory
KDDI Research, Inc.
2-1-15 Ohara, Fujimino-shi, Saitama, Japan
email: ro-saha@kddi-research.jp

***Abstract*—In this paper, we propose a hybrid interweave-underlay spectrum access technique to share the licensed 28 GHz millimeter-wave spectrum of one Mobile Network Operator (MNO), termed as primary MNO, with small cells in a building of another MNO, termed as secondary MNO, in a country. The proposed technique explores the traditional interweave spectrum access technique by operating a small cell at the maximum transmission power if no user equipment of a primary MNO exists and the traditional underlay spectrum access technique by operating a small cell at a reduced transmission power if a user equipment of a primary MNO exists within the coverage of any in-building small cell of a secondary MNO. We derive average capacity, spectral efficiency, and energy efficiency and carry out extensive numerical and simulation results and analyses for a secondary MNO of a country consisting of four MNOs. It is shown that the proposed technique can improve the spectral efficiency by about 2.82 times, and the energy efficiency by about 73% of the secondary MNO as compared to that of the traditional static licensed spectrum allocation technique that allocates each MNO an equal amount of the 28 GHz millimeter-wave spectrum. Moreover, we show that the proposed technique can satisfy the expected spectral efficiency and energy efficiency requirements for Sixth-Generation (6G) mobile systems by reusing the millimeter-wave spectrum of the secondary MNO to its small cells of roughly 31%, 36%, and 72% less number of buildings than that required by the traditional interweave, underlay, and static licensed spectrum allocation techniques, respectively.**

Keywords—6G; 28 GHz; cognitive radio; CRN; millimeter-wave; interweave; underlay; hybrid; mobile system; spectrum access.

I. INTRODUCTION

Nowadays, radio spectrum scarcity has become a major issue in mobile communications due to a non-dynamic or static allocation of spectrum to Mobile Network Operators (MNOs) to serve an ever-increasing user demand for high data rates and capacity. Such static allocations of spectrum cause a great portion of the spectrum to be left unused in time, frequency, and space, resulting in poor spectrum utilization. According to the Federal Communications Commission (FCC), the spectrum utilization below 3 GHz changes considerably with an occupancy of around 15% to 85% [1]. Recently, Cognitive Radio (CR) has been considered as a key enabling technology to address this spectrum scarcity issue [2]. In CR, spectrum access is a major function [3], which prevents collisions between primary User Equipments (UEs) and Secondary UEs (SUs) in accessing any spectrum. In this regard, interweave and underlay are two major spectrum access categories in CR.

In interweave access, SUs can opportunistically access only the spectrum not used by Primary UEs (PUs). Though interweave access needs additional spectrum sensing by SUs to find an idle spectrum of PUs, SUs are allowed to transmit at the maximum power. In contrast, in underlay access, SUs can simultaneously access the spectrum of PUs subject to satisfying the interference threshold set by PUs. Though underlay access suffers from the reduced transmission power of SUs to limit Co-Channel Interference (CCI) to PUs, no spectrum sensing is needed by SUs. Hence, though both interweave and underlay have pros and cons as aforementioned, the combination of these two spectrum accesses can maximize the Spectral Efficiency (SE) and Energy Efficiency (EE) [4]. More specifically, SUs can explore the interweave access when the spectrum of PUs is idle and the underlay access when the spectrum of PUs is busy. This allows SUs to operate at the maximum power during an idle period in contrast to operating at reduced power when employing only the underlay access all the time.

A number of research works have addressed the hybrid or joint interweave-underlay spectrum access. For example, Khan et al. [5] have proposed a hybrid underlay-interweave mode enabled Cognitive Radio Network (CRN) scheme. Likewise, in [6], Zoe et al. have proposed a hybrid interweave-underlay spectrum access scheme using spectrum sensing in the 5 GHz license-exempt spectrum. Besides, for the performance analysis, Mehmeti et al. [2] have provided expressions that allow the performance comparison of the interweave and underlay modes under a unified network setup. Also, in [7], Jazaie et al. have presented the downlink capacity region of a secondary network in a multiuser spectrum sharing system for a hybrid underlay-interweave paradigm. However, a consensus about the more suitable spectrum access out of the interweave and underlay for SUs is not too obvious [2].

Besides, most data are originated in indoors, particularly in dense urban areas where the existence of a large number of multistory buildings installed with small cells is an obvious scenario [8]. Hence, addressing high capacity and data rates in such buildings is crucial. In this regard, due to the favorable propagation characteristics of high-frequency millimeter-wave (mmWave) signals, such as low interference effects and the existence of Line-of-Sight (LOS) components, operating small cells at the mmWave spectrum in such buildings can be a promising candidate to provide high data rates and capacity. In line with this, a hybrid interweave-underlay spectrum access technique for sharing the licensed mmWave spectrum of one MNO with in-building small cells of another to increase its available spectrum within multistory buildings can play a vital role in serving high capacity and data rates indoors, which, however, has not been addressed in the existing literature.

 ISBN: 978-1-61208-828-0

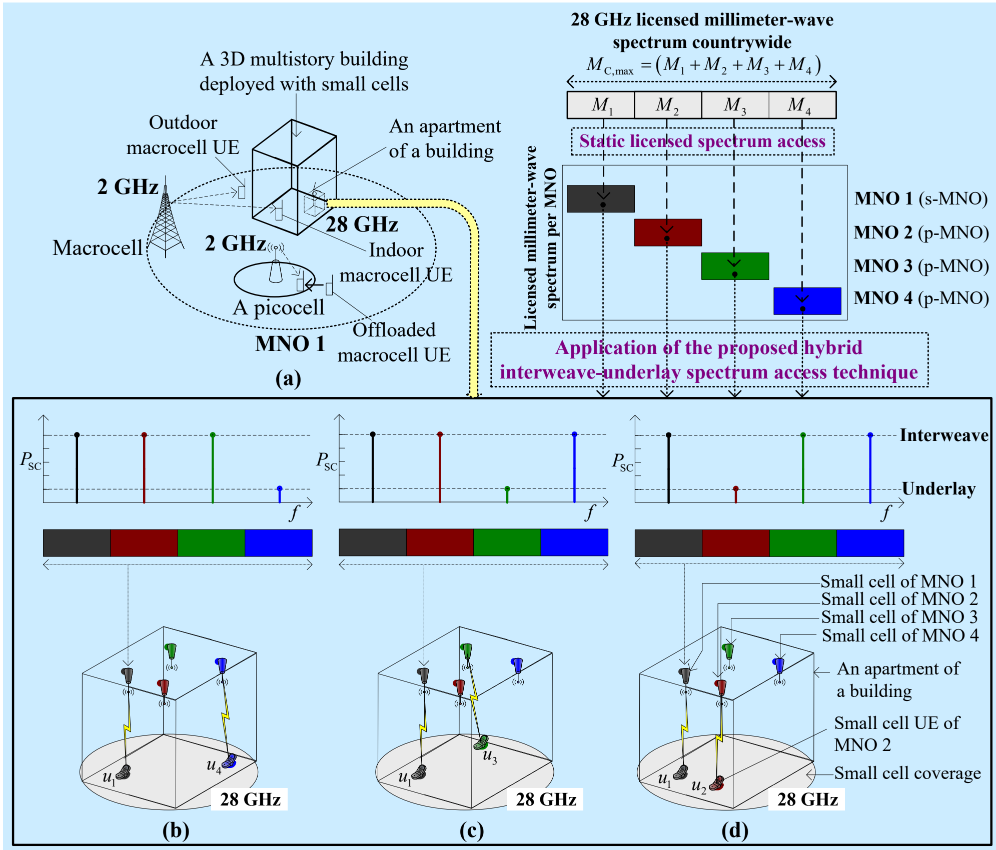

Figure 1. A system architecture consisting of four MNOs in a country. P_{SC} denotes the transmission power of an in-building small cell base station of MNO 1.

To address the issues outlined above, in this paper, we propose a hybrid interweave-underlay spectrum access technique to share the licensed 28 GHz mmWave spectrum of one MNO, referred to as primary MNO (p-MNO), with small cells in a building of another MNO, referred to as secondary MNO (s-MNO), in a country. The proposed technique explores both the traditional interweave and underlay spectrum access techniques. The following are performed section-wise to address the proposed technique. In Section II, the proposed technique along with the system architecture are presented. In Section III, we perform relevant mathematical analysis to derive average capacity, SE, and EE performance metrics for s-MNOs by employing the proposed technique. Section IV provides default simulation parameters and assumptions, as well as extensive numerical and simulation results and analyses for an s-MNO of a country consisting of four MNOs to demonstrate that the proposed technique can satisfy both the SE and EE requirements for Sixth-Generation (6G) mobile systems. We conclude the paper in Section V.

II. System Architecture and Proposed Technique

A. System Architecture

We consider that four MNOs (i.e., MNO 1, MNO 2, MNO 3, and MNO 4) are operating in a country. Assume that each MNO has a similar system architecture consisting of three types of Base Stations (BSs), namely Macrocell BSs (MBSs), Picocell BSs (PBSs), and Small Cell BSs (SBSs). For simplicity, we show the detailed architecture of only one MNO (i.e., MNO 1) in Figure 1(a). All SBSs are deployed only within 3-Dimensional (3D) multistory buildings each serving one UE at a time. Both in-building SBSs and PBSs are located within the coverage of an MBS. Each macrocell UE of an MBS is served either by the MBS itself or by any PBSs within its coverage. SBSs within each building are considered to be operating at the 28 GHz mmWave spectrum, whereas MBSs and PBSs are operating at the 2 GHz spectrum (Figure 1(a)).

We assume that each MNO is given a license for an equal amount of 28 GHz mmWave spectrum, and the spectrum of one MNO can be shared with in-building SBSs of another MNO following a hybrid interweave-underlay spectrum access technique presented in the following section. Figures 1(b)-1(d) show an example for sharing the spectra of MNO 2, MNO 3, and MNO 4 as p-MNOs with an in-building SBS of MNO 1 as an s-MNO using the proposed technique by considering that the maximum of two UEs (one from MNO 1 and the other from any p-MNO) can exist simultaneously within the coverage of the SBS.

B. Proposed Technique

We propose a hybrid interweave-underlay spectrum access technique for the dynamic spectrum access of the licensed 28-GHz mmWave spectrum of one MNO to another in a country, stated as follows.

"The licensed 28-GHz mmWave spectrum of one MNO (i.e., p-MNO) can be allowed to share with small cells in a building of another MNO (i.e., s-MNO) subject to operating each small cell of the s-MNO at the maximum transmission power if no UE of the p-MNO is present, but at a reduced transmission power if a UE of the p-MNO is present. The reduced transmission power is varied in accordance with the predefined interference threshold set by the p-MNO."

As indicated above, the proposed technique takes advantage of exploring both the interweave as well as underlay spectrum access techniques. Using the interweave access, small cells of an s-MNO in a building can access opportunistically the whole licensed 28-GHz spectrum of every single p-MNO in a country in time, frequency, and space by operating them at the maximum transmission power as long as no UE of the respective p-MNO is present at the same time. But, if a UE of any p-MNO is present, following the underlay access, each small cell of the s-MNO immediately reduces its transmission power corresponding to the predefined interference threshold set by the p-MNO to limit CCI to the UE of the p-MNO. In this regard, the small cells of the s-MNO keep sensing to detect the presence of UEs for each p-MNO to update the corresponding spectrum access mode of operation to either the interweave access or the underlay access such that the CCI constraint to UEs of the respective p-MNO can be guaranteed. More specifically, each small cell of an s-MNO needs to switch only between two states of its transmission power, either the maximum or the reduced one. For switching, both reactive and proactive spectrum sensing approaches can be applied to detect the usage of the shared spectrum of any p-MNO. In the reactive approach, an s-MNO performs spectrum sensing mechanisms to detect the usage on the shared spectrum, whereas in the reactive approach, based on the knowledge of the traffic model of the UEs of a p-MNO, the arrival of UEs can be predicted [9] to reduce the transmission power beforehand.

III. Mathematical Analysis

Assume that O denotes the maximum number of MNOs of a country such that $o \in \boldsymbol{O} = \{1,2,...,O\}$. Let $M_{\text{C,max}}$ denote the countrywide 28 GHz mmWave spectrum defined in terms of the number of Resource Blocks (RBs), where an RB is equal to 180 kHz. Let M_o denote the amount of 28 GHz spectrum of an MNO such that $\sum_{o=1}^{O} M_o \le M_{\text{C,max}}$. Assume that L denotes the number of buildings per macrocell such that $l \in \{1,2,...,L\}$. Let S_{F} denote the number of small cells per 3D building such that $s \in \{1,2,...,S_{\text{F}}\}$, where S_{F} is assumed the same for all buildings. Let S_{M} denote the number of macrocells and let S_{P} denote the number of picocells per macrocell of each MNO. Also, let $\boldsymbol{T}$ denote the simulation run time with the maximum time of Q (in time step each lasting 1 ms) such that $\boldsymbol{T} = \{1, 2, 3,\ldots,Q\}$.

Denote P_{MC} and P_{PC}, respectively, as the transmission power of a macrocell and a picocell. Let $P_{\text{SC,lic},o}$ denote the transmission power of an SBS when operating at the licensed spectrum of its MNO o, whereas $P_{\text{SC,int},o}$ and $P_{\text{SC,und},o}$ denote, respectively, the transmission power of an SBS of MNO o when operating at the shared spectrum of other MNOs $\boldsymbol{O} \backslash o$ under the interweave and underlay spectrum access techniques. Let $P_{\text{SC,max},o}$ and $P_{\text{SC,red},o}$ denote, respectively, the maximum transmission power and the reduced transmission power of an SBS of MNO o when operating under the interweave and underlay spectrum access techniques such that $P_{\text{SC,max},o} > P_{\text{SC,red},o}$. Let $I_{\text{thr,und}}$ denote the predefined value of the maximum CCI that can be caused by an SBS to a UE of a p-MNO when operating under the underlay spectrum access technique. If κ denotes the interference channel gain, then the transmission power of an SBS of MNO o when operating under the underlay access can be adapted with $I_{\text{thr,und}}$ as follows [10].

$$P_{\text{SC,und},o} = \begin{cases} P_{\text{SC,red},o}, & \left(\kappa P_{\text{SC,red},o}\right) \le I_{\text{thr,und}} \\ \left(I_{\text{thr,und}}/\kappa\right), & \left(\kappa P_{\text{SC,red},o}\right) > I_{\text{thr,und}} \end{cases} \quad (1)$$

The received Signal-to-Interference-Plus-Noise Ratio (SINR) at RB=i in Transmission Time Interval (TTI)=t at a UE of an MNO o can be expressed as

$$\rho_{t,i,o} = \left(P_{t,i,o} / (N^{\text{s}}_{t,i,o} + I_{t,i,o})\right).H_{t,i,o} \quad (2)$$

where $P_{t,i,o}$ is the transmission power, $N^{\text{s}}_{t,i,o}$ is the noise power, $I_{t,i,o}$ is the total interference signal power, and $H_{t,i,o}$ is the link loss for a link between a UE and a BS of an MNO o at RB=i in TTI=t. $H_{t,i,o}$ can be expressed in dB as

$$H_{t,i,o}(\text{dB}) = (G_{\text{t}} + G_{\text{r}}) - (L_{\text{F}} + PL_{t,i,o}) + (LS_{t,i,o} + SS_{t,i,o}) \quad (3)$$

where $(G_{\text{t}} + G_{\text{r}})$ and L_{F} are, respectively, the total antenna gain and connector loss. $LS_{t,i,o}$, $SS_{t,i,o}$, and $PL_{t,i,o}$, respectively, denote large scale shadowing effect, small scale Rayleigh or Rician fading, and distance-dependent path loss between a BS and a UE of an MNO o at RB=i in TTI=t.

Using Shannon's capacity formula, a link throughput at RB=i in TTI=t for an MNO o in bps per Hz is given by [11] [12]

$$\sigma_{t,i,o}\left(\rho_{t,i,o}\right) = \begin{cases} 0, & \rho_{t,i,o} < -10\,\text{dB} \\ \beta \log_2\left(1 + 10^{(\rho_{t,i,o}(\text{dB})/10)}\right), & -10\,\text{dB} \le \rho_{t,i,o} \le 22\,\text{dB} \\ 4.4, & \rho_{t,i,o} > 22\,\text{dB} \end{cases} \quad (4)$$

where β denotes the implementation loss factor.

Let $M_{\text{MBS},o}$ denote the 2 GHz spectrum in RBs of a macrocell for an MNO o. Then, the total capacity of all macrocell UEs for an MNO o can be expressed as

$$\sigma_{\text{MBS},o} = \sum_{t=1}^{Q} \sum_{i=1}^{M_{\text{MBS},o}} \sigma_{t,i,o}\left(\rho_{t,i,o}\right) \quad (5)$$

where σ and ρ are responses over $M_{\text{MBS},o}$ RBs of all macro UEs in $t \in \boldsymbol{T}$ for an MNO o.

Assume that each MNO o has an SBS in each apartment, and each SBS can serve the maximum of one UE at a time. Assume that there are 4 MNOs in a country such that $o \in \boldsymbol{O} = \{1,2,3,4\}$. So, a maximum of four different UEs each from one MNO may exist at once in an apartment. Each UE has two states for existence (i.e., a UE of an MNO may either exist or not) in an apartment. Let the binary digits 1 and 0 denote, respectively, the existence and nonexistence of a UE of an MNO o in an apartment such that four UEs can coexist in an apartment in a maximum of 2^4 possible ways, as shown in Table I.

Assume that the existence of four UEs in an apartment for each possible way shown in Table I is equally likely. Hence, given the existence (i.e., the binary state 1) of a UE of an MNO o (i.e., an s-MNO) over the observation time of $|\boldsymbol{T}| = Q$, UEs of other MNOs $\boldsymbol{O}\backslash o$ (i.e., p-MNOs) can coexist with the UE of MNO o in a maximum of eight possible ways, as shown in Table I, each occurs with a probability of $1/8$ and, hence, persisting for $Q/8$ during the observation time Q in an apartment.

For example, for a UE u_1 of MNO 1 as an s-MNO, all the possible combinations in which u_1 can coexist with other UEs u_2, u_3, and u_4 of MNO 2, MNO 3, and MNO 4 as p-MNOs, respectively, are the following $\{u_1\}$, $\{u_1,u_2\}$, $\{u_1,u_3\}$, $\{u_1,u_4\}$, $\{u_1,u_2,u_3\}$, $\{u_1,u_2,u_4\}$, $\{u_1,u_3,u_4\}$, and $\{u_1,u_2,u_3,u_4\}$, where each occurs with a probability of $1/8$ in an apartment. Assume that each MNO is allocated to an equal amount of spectrum of M RBs. Then, the above possible combinations for the coexistence of u_1 with other UEs (i.e., u_2, u_3, and u_4) in an apartment correspond to the amount of shared spectrum for u_1 of 3*M*, 2*M*, 2*M*, 2*M*, *M*, *M*, *M*, and 0, respectively, for the interweave access, and of 0, *M*, *M*, *M*, 2*M*, 2*M*, 2*M*, and 3*M* for the underlay access, as shown in Table I. These correspond to the total spectrum for u_1 of 4*M*, 3*M*, 3*M*, 3*M*, 2*M*, 2*M*, 2*M*, and *M,* respectively, for the interweave access, and of *M*, 2*M*, 2*M*, 2*M*, 3*M*, 3*M*, 3*M*, and 4*M* for the underlay access.

Now, if all SBSs in each building serve simultaneously in $t \in \boldsymbol{T}$, using Table I, the aggregate capacity served by an SBS of an MNO o (i.e., an s-MNO) can be found as follows. Let $P_{\text{SC,int,RB}}$ and $P_{\text{SC,und,RB}}$ denote, respectively, the transmission power per RB of an SBS of an MNO o when operating under the interweave and underlay spectrum access techniques. Assume that $\rho_{t,i,o,\text{int}}$ and $\rho_{t,i,o,\text{und}}$ denote, respectively, the received SINR at RB=i in TTI=t at a UE of an MNO o when operating at the power of $P_{t,i,o} = P_{\text{SC,int,RB}}$ under the interweave access and $P_{t,i,o} = P_{\text{SC,und,RB}}$ under the underlay access. Let $\sigma_{t,i,o,\text{int}}$ and $\sigma_{t,i,o,\text{und}}$ denote, respectively, the link throughput corresponding to $\rho_{t,i,o,\text{int}}$ and $\rho_{t,i,o,\text{und}}$. Using (2) and (4), the capacity served by an SBS of an MNO o using the interweave access at the shared spectrum of MNOs $\boldsymbol{O}\backslash o$ in $t \in \boldsymbol{T}$ is given by

$$\sigma_{s,o,\text{int}} = \begin{pmatrix} \left(3\sum_{t=1}^{(Q/8)}\sum_{i=1}^{M}\sigma_{t,i,o,\text{int}}\left(\rho_{t,i,o,\text{int}}\right)\right) \\ +\left(3\sum_{t=1}^{(Q/8)}\sum_{i=1}^{2M}\sigma_{t,i,o,\text{int}}\left(\rho_{t,i,o,\text{int}}\right)\right) \\ +\sum_{t=1}^{(Q/8)}\sum_{i=1}^{3M}\sigma_{t,i,o,\text{int}}\left(\rho_{t,i,o,\text{int}}\right) \end{pmatrix} \tag{6}$$

Also, the capacity served by an SBS of an MNO o using the underlay access at the shared spectrum in $t \in \boldsymbol{T}$ is given by

$$\sigma_{s,o,\text{und}} = \begin{pmatrix} \left(3\sum_{t=1}^{(Q/8)}\sum_{i=1}^{M}\sigma_{t,i,o,\text{und}}\left(\rho_{t,i,o,\text{und}}\right)\right) \\ +\left(3\sum_{t=1}^{(Q/8)}\sum_{i=1}^{2M}\sigma_{t,i,o,\text{und}}\left(\rho_{t,i,o,\text{und}}\right)\right) \\ +\sum_{t=1}^{(Q/8)}\sum_{i=1}^{3M}\sigma_{t,i,o,\text{und}}\left(\rho_{t,i,o,\text{und}}\right) \end{pmatrix} \tag{7}$$

Now, the capacity served by an SBS of an MNO o at the licensed spectrum of M of MNO o itself in $t \in \boldsymbol{T}$ is given by

$$\sigma_{s,o,\text{lic}} = \sum_{t=1}^{Q}\sum_{i=1}^{M}\sigma_{t,i,o,\text{lic}}\left(\rho_{t,i,o,\text{lic}}\right) \tag{8}$$

TABLE I. CO-EXISTENCE AND SHARED SPECTRUM FOR UE u_1 OF MNO 1 USING THE PROPOSED TECHNIQUE.

u_1	u_2	u_3	u_4	Shared spectrum for u_1		Licensed spectrum for u_1
				Interweave	Underlay	Both interweave and underlay
0	0	0	0	Not applicable due to the nonexistence of u_1		
0	0	0	1			
0	0	1	0			
0	0	1	1			
0	1	0	0			
0	1	0	1			
0	1	1	0			
0	1	1	1			
1	0	0	0	3*M*	0	*M*
1	0	0	1	2*M*	*M*	*M*
1	0	1	0	2*M*	*M*	*M*
1	0	1	1	*M*	2*M*	*M*
1	1	0	0	2*M*	*M*	*M*
1	1	0	1	*M*	2*M*	*M*
1	1	1	0	*M*	2*M*	*M*
1	1	1	1	0	3*M*	*M*

Based on the above, the overall aggregate capacity served by an SBS of an MNO o using the proposed technique at the licensed spectrum of M of MNO o itself, as well as the shared spectrum of MNOs $\boldsymbol{O}\backslash o$, in $t \in \boldsymbol{T}$ is given by

$$\sigma_{s,o,\text{prop}} = \left(\sigma_{s,o,\text{lic}} + \sigma_{s,o,\text{int}} + \sigma_{s,o,\text{und}}\right) \tag{9}$$

Now, the aggregate capacity served by all SBSs of an MNO o in a building using the proposed technique in $t \in \boldsymbol{T}$ is given by

$$\sigma_{S_{\text{F}},o,\text{prop}} = \sum_{s=1}^{S_{\text{F}}}\sigma_{s,o,\text{prop}} \tag{10}$$

However, due to the short distance between a small cell UE and its SBS and a low transmission power of an SBS, we assume similar indoor signal propagation characteristics for all L buildings per macrocell for an MNO o. Then, by linear approximation, the system-level average capacity, SE, and EE for an MNO o are given for L>1, respectively as follows.

$$\sigma^{\text{sys}}_{\text{cap},o,\text{prop}}\left(L\right) = \sigma_{\text{MBS},o} + \left(L\,\sigma_{S_{\text{F}},o,\text{prop}}\right) \tag{11}$$

$$\sigma^{\text{sys}}_{\text{SE},o,\text{prop}}\left(L\right) = \sigma^{\text{sys}}_{\text{cap},o,\text{prop}}\left(L\right) \Big/ \left(\left(M_{\text{MBS},o} + M\right)Q\right) \tag{12}$$

$$\sigma^{\text{sys}}_{\text{EE},o,\text{prop}}(L) = \left(\left(\left(L S_{\text{F}}\right)\left(P_{\text{SC,lic},o} + \left(1.5\left(P_{\text{SC,int},o} + P_{\text{SC,und},o}\right)\right)\right)\right) + \left(S_{\text{P}} P_{\text{PC}}\right) + \left(S_{\text{M}} P_{\text{MC}}\right)\right) \Big/ \left(\sigma^{\text{sys}}_{\text{cap},o,\text{prop}}(L)/Q\right) \quad (13)$$

Also, in the traditional Static Licensed Spectrum Allocation (SLSA) technique, each MNO is licensed exclusively for an equal amount of the 28 GHz mmWave spectrum of M RBs. Then, for SLSA, the system-level average capacity, SE, and EE for an MNO o for L>1 are given, respectively by

$$\sigma^{\text{sys}}_{\text{cap},o,\text{SLSA}}(L) = \sigma_{\text{MBS},o} + \left(L\,\sigma_{S_{\text{F}},o,\text{SLSA}}\right) \quad (14)$$

where $\sigma_{S_{\text{F}},o,\text{SLSA}} = \sum_{s=1}^{S_{\text{F}}} \sum_{t \in \boldsymbol{T}} \sum_{i=1}^{M} \sigma_{s,t,i,o}\left(\rho_{s,t,i,o}\right)$ (15)

$$\sigma^{\text{sys}}_{\text{SE},o,\text{SLSA}}(L) = \sigma^{\text{sys}}_{\text{cap},o,\text{SLSA}}(L) \Big/ \left(\left(M_{\text{MBS},o} + M\right)Q\right) \quad (16)$$

$$\sigma^{\text{sys}}_{\text{EE},o}(L) = \left(\left(L S_{\text{F}} P_{\text{SC}}\right) + \left(S_{\text{P}} P_{\text{PC}}\right) + \left(S_{\text{M}} P_{\text{MC}}\right)\right) \Big/ \left(\sigma^{\text{sys}}_{\text{cap},o,\text{SLSA}}(L)/Q\right) \quad (17)$$

From here, the improvement factors for capacity, SE, and EE performances due to applying the proposed technique for an MNO o (i.e., an s-MNO) with respect to that due to applying the SLSA technique can be expressed, respectively as follows.

$$\sigma^{\text{sys}}_{\text{cap},o,\text{IF}}(L) = \sigma^{\text{sys}}_{\text{cap},o,\text{prop}}(L) \Big/ \sigma^{\text{sys}}_{\text{cap},o,\text{SLSA}}(L) \quad (18)$$

$$\sigma^{\text{sys}}_{\text{SE},o,\text{IF}}(L) = \sigma^{\text{sys}}_{\text{SE},o,\text{prop}}(L) \Big/ \sigma^{\text{sys}}_{\text{SE},o,\text{SLSA}}(L) \quad (19)$$

$$\sigma^{\text{sys}}_{\text{EE},o,\text{IF}}(L) = \sigma^{\text{sys}}_{\text{EE},o,\text{prop}}(L) \Big/ \sigma^{\text{sys}}_{\text{EE},o,\text{SLSA}}(L) \quad (20)$$

IV. PERFORMANCE RESULT AND ANALYSIS

Table II shows the default simulation parameters and assumptions used for evaluating the performance of the proposed technique for MNO 1, as an s-MNO. For the underlay access, we assume that the transmission power of an SBS is upper limited by 20% of its maximum power. To allow flexibility in switching between the interweave and underlay accesses, for each SBS, a separate transceiver is assumed to operate at the shared spectrum of M RBs of each p-MNO.

Figure 2 shows improvement factors in terms of SE and EE performances for MNO 1 due to applying the proposed hybrid interweave-underlay technique, as well as the traditional interweave and underlay techniques. It can be found that the proposed hybrid technique improves both the SE and EE metrics of MNO 1 considerably as compared to that of the traditional interweave and underlay techniques when applied separately. This is because, using Table I, the maximum amount of the shared spectrum obtained by employing the proposed technique is 3 times (interweave and underlay techniques each contributing 1.5 times) the spectrum of MNO 1 of M RBs for any observation time Q. This causes the proposed technique to increase the licensed spectrum of M RBs to 4M RBs for MNO 1 in time Q. Since the capacity, and hence SE, is directly proportional, whereas the EE is inversely proportional, to the spectrum, the proposed technique improves SE by about 2.82 times, whereas EE by about 73%, of MNO 1, as shown in Figure 2.

Figures 3(a) and 3(b) show, respectively, the SE and EE responses for MNO 1 by reusing the mmWave spectrum of MNO 1 to its small cells in each building due to applying the proposed technique, as well as the traditional interweave, underlay, and SLSA techniques for a number of buildings of small cells. It can be found that, with an increase in l, SE increases linearly, whereas EE improves negative exponentially for all techniques, and the proposed technique outperforms all techniques in terms of SE and EE.

TABLE II. DEFAULT PARAMETERS AND ASSUMPTIONS

Parameters and Assumptions	Value
Countrywide 28 GHz spectrum and number of MNOs	200 MHz and 4
28 GHz and 2 GHz spectra per MNO	50 MHz and 10 MHz
For each MNO	
E-UTRA simulation case[1,6]	3GPP case 3
Cellular layout[2], Inter-Site Distance (ISD)[1,2,6], transmission direction	Hexagonal grid, dense urban, 3 sectors per macrocell site, 1732 m, downlink
Carrier frequency[2,5,6]	2 GHz non-LOS (NLOS) for macrocells and picocells, 28 GHz LOS for all small cells
Number of cells	1 macrocell, 2 picocells, 8 small cells per building
Total BS transmission power[1] (dBm)	46 for macrocell[1,4], 37 for picocells[1], 19 (interweave) for small cells[1,3,4], and 12.01 (underlay) for small cells
Co-channel small-scale fading model[1,3,5]	Frequency selective Rayleigh for 2 GHz NLOS, none for 28 GHz LOS
Path loss: MBS and a UE[1], Outdoor macrocell UE	PL(dB)=15.3 + 37.6 $\log_{10}R$, R is in m
Path loss: MBS and a UE[1], Indoor macrocell UE	PL(dB)=15.3 + 37.6 $\log_{10}R$ + L_{ow}, R is in m and L_{ow}=20 dB
Path loss: PBS and a UE[1]	PL(dB)=140.7+36.7 $\log_{10}R$, R is in km
Path loss: SBS and a UE[1,2,5]	PL(dB)=61.38+17.97 $\log_{10}R$, R is in m
Lognormal shadowing standard deviation (dB)	8 for MBS[2], 10 for PBS[1], and 9.9 for SBS[2,5]
Antenna configuration	Single-input single-output for all BSs and UEs
Antenna pattern (horizontal)	Directional (120^0) for MBS[1], omnidirectional for PBS[1] and SBS[1]
Antenna gain plus connector loss (dBi)	14 for MBS[2], 5 for PBS[1], 5 for SBS[1,3]
UE antenna gain[2,3]; Indoor macrocell UE[1]	0 dBi (for 2 GHz), 5 dBi (for 28 GHz, Biconical horn); 35%
UE noise figure[2,3] and UE speed[1]	9 dB (for 2 GHz) and 10 dB (for 28 GHz), 3 km/hr
Picocell coverage, the total number of macrocell UEs, and macrocell UEs offloaded to all picocells[1]	40 m (radius), 30, 2/15
3D multistory building and SBS models (square-grid apartments): number of buildings, number of floors per building, number of apartments per floor, number of SBSs per apartment, area of an apartment	L, 2, 4,1, 10×10 m^2
Scheduler and traffic model[2]	Proportional Fair and full buffer
Type of SBSs	Closed Subscriber Group femtocell BSs
TTI[1] and scheduler time constant[6] (t_c)	1 ms and 100 ms
Total simulation run time	8 ms

taken [1]from [13], [2]from [14], [3]from [15], [4]from [16], from [5][17], from [6][18].

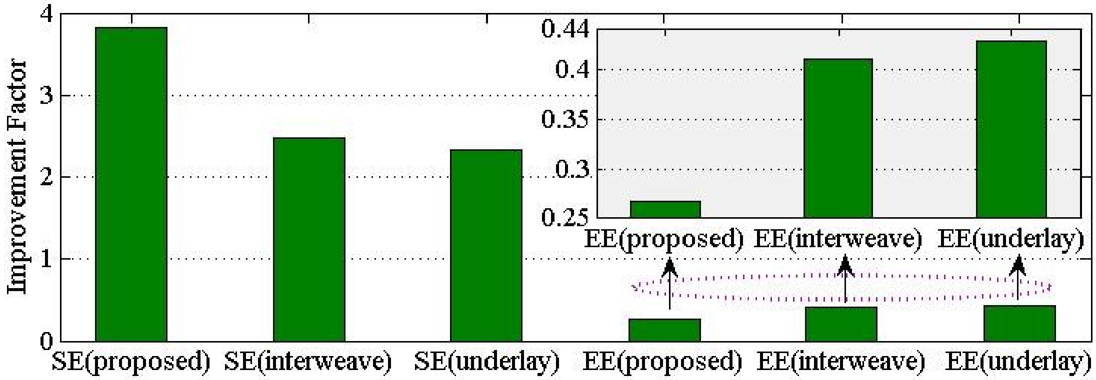

Figure 2. SE and EE improvement factors for an s-MNO (i.e., MNO 1) due to applying different techniques for a single building of SBSs.

Moreover, according to [19] [20], it is expected that the 6G mobile systems will require 10 times average SE (i.e., 270-370 bps/Hz), as well as 10 times average EE (i.e., 0.3μJ/bit), of 5G mobile systems [21]-[23]. Using Figure 3, the values of l that satisfy both SE and EE requirements for 6G mobile systems are 9, 13, 14, and 32, respectively, for the proposed hybrid, interweave, underlay, and SLSA techniques.

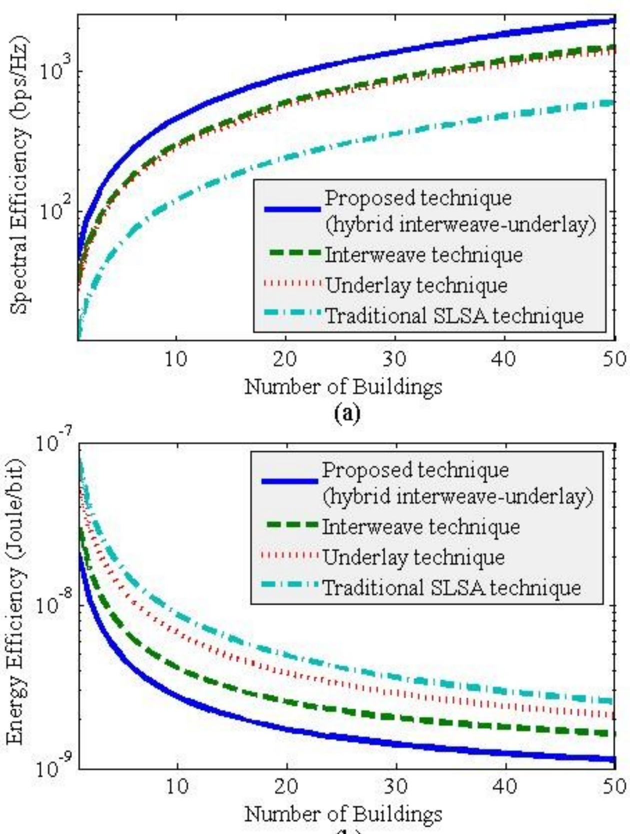

Figure 3. (a) SE and (b) EE performances for MNO 1 due to applying different techniques for multiple buildings of SBSs.

According to the evidence above, the proposed hybrid interweave-underlay technique can satisfy both SE and EE requirements for 6G mobile systems by reusing the whole mmWave spectrum of MNO 1 to its small cells of roughly 31%, 36%, and 72% less number of buildings than that required by the traditional interweave, underlay, and SLSA techniques, respectively.

V. CONCLUSION

In this paper, we have proposed a hybrid interweave-underlay spectrum access technique to share the licensed 28 GHz millimeter-wave (mmWave) spectrum of one MNO with small cells in a building of another MNO in a country. We have derived average capacity, Spectral Efficiency (SE), and Energy Efficiency (EE) performance metrics for the proposed technique and carried out extensive numerical and simulation results and analyses for MNO 1 of a country consisting of four MNOs. It has been shown that the proposed technique can improve the SE by about 2.82 times and the EE by about 73% of MNO 1 as compared to that of the traditional Static Licensed Spectrum Allocation (SLSA) technique. Further, we have shown that the proposed technique can satisfy both SE and EE requirements for 6G mobile systems by reusing the mmWave spectrum of MNO 1 to its small cells of roughly 31%, 36%, and 72% less number of buildings than that required by the traditional interweave, underlay, and SLSA techniques, respectively.

The proposed technique can be investigated further for a complete analysis to address numerous crucial issues, including millimeter-wave bands other than 28 GHz, such as 26 GHz, 38 GHz, and 60 GHz, non-LOS path loss models, directional millimeter-wave antennas, spectrum sensing mechanisms and control signaling overhead, implementation complexity analysis, burst traffic characteristics, random deployments of indoor UEs, as well as serving more than one UE simultaneously by a single small cell in a building.

REFERENCES

[1] Spectrum Policy Task Force Report. Federal Communications Commission, Washington, DC, USA, Tech. Rep. 02-155, Nov. 2002. Available Online: https://www.fcc.gov/document /spectrum-policy-task-force. [retrieved: August, 2020].

[2] F. Mehmeti and T. Spyropoulos, "Performance Analysis, Comparison, and Optimization of Interweave and Underlay Spectrum Access in Cognitive Radio Networks," IEEE Transactions on Vehicular Technology, vol. 67, pp. 7143-7157, Aug. 2018, doi: 10.1109/TVT.2018.2828090.

[3] I. F. Akiyildiz, W. Y. Lee, M. C. Vuran, and S. Mohanty, “A Survey on Spectrum Management in Cognitive Radio Networks,” IEEE Communications Magazine, vol. 46, pp. 40-48, Apr. 2008, doi: 10.1109/MCOM.2008.4481339.

[4] A. Sharmila and P. Dananjayan, “Spectrum Sharing Techniques in Cognitive Radio Networks - A Survey,” Proc. The 2019 IEEE International Conference on System, Computation, Automation and Networking (ICSCAN), Pondicherry, India, 2019, pp. 1-4.

[5] A. U. Khan et al., “HBLP: A Hybrid Underlay-Interweave Mode CRN for the Future 5G-based Internet of Things,” IEEE Access, vol. 8, pp. 63403-63420, 2020, doi: 10.1109/ACCESS.2020.2981413.

[6] P. Zuo, T. Peng, W. Linghu and W. Wang, “Optimal Resource Allocation for Hybrid Interweave-Underlay Cognitive Satcom Uplink,” Proc. The 2018 IEEE Wireless Communications and Networking Conference (WCNC), IEEE Press, 2018, pp. 1-6.

[7] M. Jazaie and A. R. Sharafat, “Downlink Capacity and Optimal Power Allocation in Hybrid Underlay–Interweave Secondary Networks,” IEEE Transactions on Wireless Communications, vol. 14, pp. 2562-2570, May 2015, doi: 10.1109/TWC.2014.2388222.

[8] R. K. Saha, “Countrywide Mobile Spectrum Sharing with Small Indoor Cells for Massive Spectral and Energy Efficiencies in 5G and Beyond Mobile Networks,” Energies, vol. 12, Art. No. 3825, Oct. 2019, doi.org/10.3390/en12203825.

[9] A. Ali and W. Hamouda, “Advances on Spectrum Sensing for Cognitive Radio Networks: Theory and Applications,” IEEE Communications Surveys & Tutorials, vol. 19, pp. 1277-1304, Second quarter 2017, doi: 10.1109/COMST.2016.2631080.

[10] J. Oh and W. Choi, “A Hybrid Cognitive Radio System: A Combination of Underlay and Overlay Approaches,” Proc. 2010 IEEE 72nd Vehicular Technology Conference - Fall, Sept. 2010, pp. 1-5.

[11] R. K. Saha, “A Hybrid System and Technique for Sharing Multiple Spectrums of Satellite Plus Mobile Systems with Indoor Small Cells in 5G and Beyond Era,” IEEE Access, vol. 7, pp. 77569-77596, 2019, doi: 10.1109/ACCESS.2019.2921723.

[12] R. K. Saha and C. Aswakul, “A Novel Frequency Reuse Technique for In-Building Small Cells in Dense Heterogeneous Networks,” IEEJ Transactions on Electrical and Electronic Engineering, vol. 13, pp. 98-111, Jan. 2018, doi.org/10.1002/tee.22503.

[13] Evolved Universal Terrestrial Radio Access (E-UTRA); Radio Frequency (RF) System Scenarios. document 3GPP TR 36.942, V.1.2.0, 3rd Generation Partnership Project, Jul. 2007. Available online: https://portal.3gpp.org/ desktopmodules /Specifications/Specification Details.aspx?specificationId=2592 [retrieved: February, 2020]

[14] Simulation Assumptions and Parameters for FDD HeNB RF Requirements. document TSG RAN WG4 (Radio) Meeting #51, R4-092042, 3GPP, May 2009. Available online: https://www.3gpp.org/ftp/tsg_ran /WG4_Radio/TSGR4_51/Documents/ [retrieved: February, 2020].

[15] Guidelines for Evaluation of Radio Interface Technologies for IMT-2020. Report ITU-R M.2412-0 (10/2017), Geneva, 2017. Available online: https://www.itu.int/dms_pub/itu-r/opb/rep/R-REP-M.2412-2017-PDF-E.pdf [retrieved: February, 2020]

[16] R. K. Saha, P. Saengudomlert, and C. Aswakul, “Evolution Toward 5G Mobile Networks-A Survey On Enabling Technologies,” Engineering Journal, vol. 20, pp. 87-119, Jan. 2016, doi.org/10.4186/ej.2016.20.1.87.

[17] G. R. Maccartney, T. S. Rappaport, S. Sun, and S. Deng, “Indoor Office Wideband Millimeter-Wave Propagation Measurements and Channel Models at 28 and 73 GHz for Ultra-Dense 5G Wireless Networks,” IEEE Access, vol. 3, pp. 2388-2424, 2015, doi: 10.1109/ACCESS.2015.2486778.

[18] R. K. Saha, S. Nanba, and K. Nishimura, “A Technique for Cloud Based Clustering and Spatial Resource Reuse and Scheduling of 3D In-Building Small Cells Using CoMP for High Capacity CRAN,” IEEE Access, vol. 6, pp. 71602-71621, Nov. 2018, doi: 10.1109/ACCESS.2018.2879835.

[19] Z. Zhang et al., “6G Wireless Networks: Vision, Requirements, Architecture, and Key Technologies,” IEEE Vehicular Technology Magazine, vol. 14, pp. 28-41, Sept. 2019, doi: 10.1109/MVT.2019.2921208.

[20] S. Chen et al., “Vision, Requirements, and Technology Trend of 6G: How to Tackle the Challenges of System Coverage, Capacity, User Data-Rate and Movement Speed,” IEEE Wireless Communications, vol. 27, no. 2, pp. 218-228, Apr. 2020, doi: 10.1109/MWC.001.1900333.

[21] C.-X. Wang et al., “Cellular Architecture and Key Technologies for 5G Wireless Communication Networks,” IEEE Communications Magazine, vol. 52, pp. 122-130, Feb. 2014, doi: 10.1109/MCOM.2014.6736752.

[22] G. Auer et al., “How Much Energy is Needed to Run a Wireless Network?” IEEE Wireless Communications, vol. 18, pp. 40-49, Oct. 2011, doi: 10.1109/MWC.2011.6056691.

[23] R. K. Saha, “3D Spatial Reuse of Multi-Millimeter-Wave Spectra by Ultra-Dense In-Building Small Cells for Spectral and Energy Efficiencies of Future 6G Mobile Networks,” Energies, vol. 13, Art. No. 1748, Apr. 2020, doi.org/10.3390/en13071748.

 ISBN: 978-1-61208-828-0